The FASEB Journal express article 10.1096/fj.01-1035fje. Published online July 18, 2002.

Androgen receptor with elongated polyglutamine tract forms aggregates that alter axonal trafficking and mitochondrial distribution in motoneuronal processes

Federica Piccioni,*,† Paolo Pinton,‡ Silvia Simeoni,*,† Paola Pozzi,*,† Umberto Fascio,§ Guglielmo Vismara,*,† Luciano Martini,*,† Rosario Rizzuto,‡ Angelo Poletti*,†

*Institute of Endocrinology, Centre of Excellence for the Study and Treatment of Neurodegenerative Diseases, University of Milan, Milan, Italy; †Centre of Excellence for the Study and Treatment of Neurodegenerative Diseases, University of Milan, Milan, Italy; ‡Interdisciplinary Center for the Study of Inflammation (ICSI) and Telethon Center for Cell Imaging (TCCI), Department of Experimental and Diagnostic Medicine, Section of General Pathology, University of Ferrara, Ferrara, Italy; and §Department of Biology, Section of Zoology and Interdepartmental Center for Advanced Microscopy, University of Milan, Milan, Italy

Corresponding author: Angelo Poletti, Istituto di Endocrinologia, Centre of Excellence for the Study and Treatment of Neurodegenerative Diseases, University of Milan, Via Balzaretti 9, 20133 Milano, Italy. E-mail: Angelo.Poletti@unimi.it

ABSTRACT

The CAG/polyglutamine (polyGln)-related diseases include nine different members that together form the most common class of inherited neurodegenerative disorders; neurodegeneration is linked to the same type of mutation, found in unrelated genes, consisting of an abnormal expansion of a polyGln tract normally present in the wild-type proteins. Nuclear, cytoplasmic, or neuropil aggregates are detectable in CAG/polyGln-related diseases, but their role is still debated. Alteration of the androgen receptor (AR), one of these proteins, has been linked to spinal and bulbar muscular atrophy, an X-linked recessive disease characterized by motoneuronal death. By using immortalized motoneuronal cells (the neuroblastoma-spinal cord cell line NSC34), we analyzed neuropil aggregate formation and toxicity: green fluorescent protein-tagged wild-type or mutated ARs were cotransfected into NSC34 cells with a blue fluorescent protein tagged to mitochondria. Altered mitochondrial distribution was observed in neuronal processes containing aggregates; occasionally, neuropil aggregates and mitochondrial concentration corresponded to axonal swelling. Neuropil aggregates also impaired the distribution of the motor protein kinesin. These data suggest that neuropil aggregates may physically alter neurite transport and thus deprive neuronal processes of factors or components that are important for axonal and dendritic functions. The soma may then be affected, leading to neuronal dysfunctions and possibly to cell death.

Key words: triplet repeats • fast axonal transport • kinesin • neurodegeneration • spinal bulbar muscular atrophy

The expression of proteins containing abnormal elongations of polyglutamine (polyGln) stretches (coded by CAG triplet repeat gene sequences of expanded size) is associated with several types of neuronal degeneration. So far, at least nine different proteins containing a polyGln tract of increased size have been cloned from patients with neurodegenerative disorders (polyGln-related diseases): Kennedy's disease or spinal and bulbar muscular atrophy (SBMA); Huntington's disease (HD); spinocerebellar ataxias (SCAs) 1, 2, 3 (or Machado-Joseph disease), 6, and 7; and dentatorubral and pallidoluysian atrophy (DRPLA) (1). The polyGln expansion of the tract present in the TATA box binding protein has recently been linked to a novel autosomal dominant cerebellar ataxia (SCA17) (2). The first identified protein of this class is the mutated androgen receptor (AR) in which the polyGln tract elongation, present in the N-terminal transactivation domain, is linked to SBMA (3, 4). This is an X-linked recessive neurodegenerative disorder characterized by selective motoneuronal loss in the anterior horn of the spinal cord and in the bulbar region; depletion of sensory neurons in the dorsal root ganglia also occurs (5). Normally, the AR polyGln repeat ranges from 9 to 34 glutamines, whereas in SBMA patients the size of the polyGln tract is expanded to be more than 35 glutamines (3, 6-9). The biological functions of the protein causing SBMA are well known, and AR activation can be measured with various functional assays (e.g., hormone binding, DNA binding, transactivation, cellular trafficking). With these tests, it has been shown that the expanded polyGln tract only partially modifies the transcriptional activity of the SBMA AR (10-14). Because patients with androgen resistance syndromes do not show signs of neurodegeneration, it is likely that the neurological phenotype of SBMA is due to a direct toxic effect of the expanded polyGln tract at the neuronal level, rather than to a defective AR function. The acquired toxicity is probably common to all proteins containing the unusually long polyGln tract.

A common feature of all polyGln-related diseases is the intracellular formation of insoluble aggregates formed by the mutated proteins in the cell nucleus and/or cytoplasm (15-38). The aggregates found in the cytoplasm are perinuclear or are localized in the cell processes (e.g., in the neurites of neuronal cells); in the latter case they have been called neuropil aggregates (20, 24, 39).

Because these inclusions are analogous to those found in other types of neurodegenerative disorders (such as Alzheimer’s, Parkinson’s, and prion diseases), it has been proposed that aggregates may be toxic for long-lived postmitotic cells. However, their pathological role is still matter of discussion, and neuronal cell death observed in polyGln-related disorders is now considered a multifactorial event. We have already reported that AR cytoplasmic aggregates do not seem to be toxic for transfected immortalized motoneuronal cells (the neuroblastoma-spinal cord cell line NSC34) (35). In fact, SBMA AR induces neuronal cell death in the absence of testosterone when cytoplasmic inclusions are not present; in contrast, cell survival is increased by androgen treatment (21, 35), which, in our system, induces the formation of cytoplasmic aggregates (40, 41). Apparently, cytoplasmic aggregates initially play a protective role for neurons, mainly by removing toxic proteins from soluble compartments in the cell (35, 42, 43).

A different role appears to be played by intranuclear inclusions. In SBMA patients, these inclusions have been observed in central nervous system regions susceptible to neurodegeneration (25, 26), and they seem to be associated with the production of a specific AR N-terminal fragment containing the elongated polyGln tract (17, 21, 44), which might start the

aggregation process into the nuclei (21, 45). The potential toxicity of nuclear aggregates may be linked to sequestration, by AR aggregates, of steroid receptor coactivator 1 (37) and of CREB binding protein, two transcriptional coactivators that are involved in a variety of cell-signaling cascades fundamental for neuronal physiology (46).

With regard to neuropil aggregates (20), they also seem to be highly correlated (at least in HD) with the development of neurological symptoms (24). In fact, it has been reported, both in HD patients (39) and in the HD transgenic mouse (24), that they are much more common than nuclear aggregates and that they appear largely before the onset of clinical symptoms. Using an in vitro motoneuronal model for SBMA (35), we also found inclusions in the neuropil. Unfortunately, we could not analyze the potential toxicity of these inclusions with standard cell viability tests, because the inclusions were present in only a limited number of transfected immortalized motoneuronal cells. Neuropil aggregates of mutated AR may play important pathogenetic roles because they may mechanically (physically) alter neurite functions by blocking the transport of organelles, vesicles, and polyribosomes along the axons, as well as by modifying the accessibility to factors that are important for the neurofilament network (47).

In the present study, we analyzed the potential neurotoxicity of neuropil aggregates by investigating axonal and dendritic transport of mitochondria in living cells expressing the mutated SBMA AR. We also analyzed possible aggregate-induced alterations of the anterograde motor protein kinesin. Our results showed that neuropil aggregates strongly affect the distribution of mitochondria in neuronal processes of living cells, a process mediated by a fast axonal transport. Neuropil aggregates also altered the distribution of the motor protein kinesin along the cell processes of immortalized motoneuronal cells.

MATERIALS AND METHODS

Reagents

Anti-androgen receptor mouse monoclonal IgG1 antibody clone F39.4.1 recognizing residues 301-320 of the N-terminal domain of the human AR was purchased from Euro-Diagnostica (Malmo, Sweden). AR (N-20), an affinity-purified rabbit polyclonal antibody raised against a synthetic peptide reproducing an amino acid sequence located in the N-terminal region of the human AR, and Actin C-2, a mouse monoclonal IgG1 antibody directed to the C terminus of actin of human origin, were obtained from Santa Cruz Biotechnology (Santa Cruz, CA). The mouse anti-kinesin monoclonal antibody (MAB1614) reacting with the heavy chain of kinesin near the N terminus was obtained from Chemicon International (Temecula, CA). Living Colors D.s. Peptide Antibody is an affinity-purified rabbit polyclonal antibody recognizing the *Discosoma* sp. red fluorescent protein (D.s. Antibody, Clontech, Palo Alto, CA).

Tetramethyl rhodamine isothiocyanate (TRITC)-conjugated AffiniPure Donkey Anti-Mouse IgG (H+L) secondary antibody was purchased from Jackson ImmunoResearch Laboratories (West Grove, PA).

Defined FBS was obtained from Hyclone Laboratories, Logan, UT. All the tissue culture reagents were from Seromed, Biochrom KG, Berlin, Germany. Charcoal-stripped FCS (CS-FCS)

was prepared as previously described (48) and used in all experiments in which steroid hormone treatments were utilized. Chemicals were obtained from Sigma, St. Louis, MO. NSC34 cells were kindly provided by Dr. Neil R. Cashman (McGill University, Montreal, Canada).

Plasmids

pEGFP-N1, pEGFP-C1, and pDsRed1-N1 were obtained from Clontech. The plasmids expressing the cDNA coding for the full-length wild-type AR (either with the normal size of the polyglutamine tract = Q22, or in which the polyGln tract was artificially removed = Q0) and mutated forms of AR (48 contiguous glutamines) were obtained as previously described (35). The green fluorescent protein (GFP)-AR fusion protein expression vectors were generated by insertion of the AR cDNA in the multiple cloning site of the pEGFP-C1, as previously described (35). In the chimeric proteins, the GFP is linked to the N-terminal region of the wild-type and mutated AR proteins.

The mtBFP plasmid has been previously described (49) and contains a pCMV promoter driving the expression of a chimeric cDNA coding for the blue fluorescent protein (BFP) fused with a portion of the cDNA of cytochrome *c* oxidase subunit VIII that encodes the mitochondrial targeting "presequence" and six amino acids of the mature protein.

Plasmids were utilized throughout the study to visualize mitochondria in living cells, by means of high-resolution inverted fluorescence microscopy.

Cell culture

The NSC34 cell lines are hybrid cell lines obtained by fusion of mouse motoneuron-enriched embryonic day 12-14 spinal cord cells (from gestational day 14-16) with mouse neuroblastoma cells (50, 51). The hybrid dispays a multipolar neuron-like phenotype and possesses most of the motoneuronal properties. The initial cell characterization, by reverse transcriptase-polymerase chain reaction (RT-PCR), demonstrated that these cells do not express endogenous mouse AR (52). The immortalized motoneurons have been routinely maintained in Dulbecco's modified Eagle's medium (DMEM) supplemented with 5% defined FBS, 1 mM glutamine, and antibiotics (penicillin G, potassium salt, Bristol-Myers Squibb [New York, NY], 100 IU/ml; and streptomycin sulfate, Squibb, 100 μg/ml) and grown at 37°C in a humidified atmosphere (5% CO_2, 95% air) in 25-cm^2 flasks (Corning, Cambridge, MA), with the medium being changed every 2-3 days. Every week the cells were detached from the plate by mechanical dissociation in culture medium and were replated at a density of 5×10^4 cells/flask. When cells were treated with testosterone, FCS was always replaced with CS-FCS (5%) to eliminate endogenous steroids.

Transient transfection

The day before transfection, NSC34 cells were plated in the six-well cell culture plates at a concentration of 4×10^4 cells/well. Cells were transfected with GFP-AR.Q0, GFP-AR.Q22, or GFP-AR.Q48 constructs; on the basis of the type of experiments performed, the full panel of plasmids was also cotransfected with mtBFP or pDsRed1-N1 using Lipofectamine Plus (GIBCO

BRL, Gaithersburg, MD). For microscopy of living cells, the cells were plated in the 6-well multiwell plate containing a round coverslip glass with a diameter of 24 mm at the same level of confluence. The day of transfection, the medium was replaced with serum-free, antibiotic-free DMEM, and then the cells were transfected according to the manufacture's procedure using different sets of plasmids (normally GFP-AR.Q0, GFP-AR.Q22, and GFP-AR.Q48 were used alone or in cotransfection with the mtBFP plasmid). After 3 h of transfection, the medium was replaced with standard growth medium containing CS-FCS. Cells were allowed to grow in these conditions for 2 or 3 days in presence or absence of a given treatment and then were used for analysis.

Western blot analysis

Transfected cells were harvested in 1% sodium dodecyl sulfate (SDS) in PBS and were briefly sonicated; protein concentration was determined by using the bicinchoninic acid method (Pierce, Rockford, IL). Western immunoblot analysis was done by SDS-polyacrylamide gel electrophoresis (PAGE) resolution of the samples obtained from NSC34/GFP-AR.Q0, NSC34/GFP-AR.Q22, and NSC34/GFP-AR.Q48 cells in the presence or absence of 1 μM testosterone. Samples of 35 μg of each lysate were heated to 100°C for 5 min in sample buffer (0.6 g/100 ml Tris, 2 g/100 ml SDS, 10% glycerol, 1% β-mercaptoethanol, pH 6.8) and loaded onto 10% SDS-PAGE gel, after which they were electrotransferred to nitrocellulose membranes (Hybond-ECL) by using a liquid transfer apparatus (Bio-Rad Laboratories, Hercules, CA) (to analyze D.s Red fluorescent protein, samples were revolved on 12% SDS). Nitrocellulose membranes were treated with a blocking solution containing 1% BSA in PBS for 1 h to block specific protein binding sites and were then incubated with the primary antibody AR (N-20) for 1 h at room temperature. Immunoreactivity was detected using the secondary antibody peroxidase-conjugated goat anti-rabbit IgG and was visualized using the enhanced chemiluminescence detection kit reagents (ECL, Amersham, Little Chalfont, Buckinghamshire, England).

The same membranes were then processed to detect the levels of actin and/or the red fluorescent protein in the samples loaded on the gel. For this purpose, primary and secondary antibodies were removed from the membrane by incubation for 30 min in stripping buffer (100 mM 2-mercaptoethanol, 2% SDS, 62.5 mM Tris-HCl, pH 6.7) at 50°C and then washing twice with 0.2% Tween 20 in PBS. The membranes were processed as described above using as primary antibody Actin C-2 to detect total actin or the D.s. antibody to detect red fluorescent protein, and as secondary antibody peroxidase-conjugated goat anti-mouse IgG.

Immunofluorescence analysis

Cells were plated on noncoated glass coverslips before transfection. At 72 h after transfection, the cells were fixed for 10 min at room temperature in 4% paraformaldehyde in 0.1 M phosphate buffer, pH 7.4 (PB). Cells were permeabilized with 0.2% Triton X-100 in PBS for 20 min at room temperature. The coverslips were then blocked in PBS, 1.5% horse serum, and 0.1% Triton X-100 for 20 min. Cells were incubated overnight at 4°C with the primary antibody diluted in PBS with 0.1% Triton X-100 for mouse anti-kinesin monoclonal antibody. Coverslips were washed three times for 10 min each with 0.1% Triton X-100 in PBS and were then incubated

with rhodamine-TRITC-conjugated secondary antibody for 1 h at room temperature, washed with PBS, and mounted on slides in 9:1 glycerol/PBS.

Routine fluorescein isothiocyanate (FITC) filters were used to detect GFP, and a TRITC-conjugated secondary antibody was used to detect the kinesin.

Microscopy

To routinely analyze the transfection efficiency in living immortalized motoneuronal cells, and to measure the number and size of aggregates in the cell cytoplasm and in the neurites, we used a Zeiss axiovert microscope equipped with FITC filters for fluorescence analysis. The number of cells bearing aggregates was estimated at 32 × magnification. In the studies performed with the mtBFP protein:GFP-AR chimera transfection in living NSC34 cells, a Nikon Eclipse TE300 microscope (Nikon, Tokyo, Japan) equipped with epifluorescence and a piezoelectric motorization of the objective (Physik Instrumente, GmbH, Karlsrue/Palmbach, Germany) was used. The light field or fluorescence images were captured by a back-illuminated CCD camera (Princeton Scientific Instruments, Trenton, NJ) and were processed using Metamorph software (Universal Imaging, Downingtown, PA).

Confocal microscopy

Cells analyzed for immunoreactivity to the anti-kinesin antibody were counterstained with the TRITC-conjugated secondary antibody and were then visualized by use of a Leica TCS-NT (Leica Microsystem, Heidelberg, Germany) confocal laser scanning microscope equipped with an argon/krypton laser and 75 mW multiline. Focal series of horizontal planes of sections were simultaneously monitored for GFP and rhodamine, using the 488- and 568-nm laser line, a band pass 590/30-nm filter, and a long pass 590-nm filter.

RESULTS

NSC34 is a mouse hybrid cell line obtained by the fusion of mouse motoneuron-enriched embryonic day 12-14 spinal cord cells with mouse neuroblastoma cells (50, 51). The hybrid displays a multipolar neuronal-like aspect, which has been fully characterized for its motoneuronal phenotype (50, 51), and does not express endogenous mouse AR (52). This cell line is routinely used in our laboratory in transfection experiments to analyze the effect of wild-type and mutated ARs in immortalized motoneurons.

Cellular model for the study of spinal and bulbar muscular atrophy

Figure 1 provides a schematic representation of the ARs containing polyGln tracts of different sizes the GFP-AR.[Q(n)] chimeras utilized throughout the study. The GFP-AR.Q(n) expression is driven by the potent cytomegalovirus (CMV) promoter. GFP-AR.Q0 expresses an AR cDNA in which the CAG repeat was artificially removed (there is no polyGln tract in the AR protein); the GFP-AR.Q22 represents the wild-type AR, with a polyGln tract of 22 glutamines; and the GFP-AR.Q48 expresses AR with an elongated polyGln tract of 48 contiguous glutamines. No additional amino acid changes were present, as determined by sequence analysis. These plasmids

were used in transient transfections of NSC34 cells, and the expression of the desired cDNAs was tested by RT-PCR analysis followed by Southern analysis (data not shown). All clones expressed high levels of AR mRNA, and the size of the CAG expansion in NSC34/GFP-AR.Q48 remained stable, indicating that no rearrangement of the expanded tract had occurred in this cell model.

Figure 2 shows a representative Western blot analysis performed on total cellular extracts of NSC34 cells cotransfected with recombinant GFP-AR.Q(n) and pDsRed1-N1, which codes for a protein utilized as internal control. The different GFP-AR proteins (upper panel) were of the size expected and showed an increment in the molecular weight proportional to the different polyGln tracts present in the AR. The levels of AR immunoreactivity were comparable in samples derived from untreated cells expressing GFP-AR.Q0 and Q22 (lanes 1 and 3, respectively), whereas in cells expressing GFP-AR.Q48 (lane 5) the total amount of AR protein was apparently reduced. The rate of transfection efficiency, assayed with red fluorescent protein produced by the pDsRed1-N1 (lower panel), was comparable in all samples. Testosterone treatment (lanes 2, 4, and 6) produced an increase in the immunoreactive AR protein levels. It remains to be determined whether this increase is due to transcription/translation alteration or rather to a protein stabilization mechanism, as already reported for AR (53). It is also possible that the association of the AR with DNA, which occurs in the nuclear compartment, prevents proteolysis and inhibits the degradation of the AR protein.

Dynamics of aggregate formation in immortalized motoneuronal cells

Figure 3 shows the cellular distribution of GFP-AR.Q(n) in our immortalized motoneuronal system either in the absence (Fig. 3*A*, *C*, *E*) or in the presence (Fig. 3*B*, *D*, *F*) of testosterone. It is clear that all the unliganded GFP-AR.Q(n)s (Fig. 3*A*, Q0; Fig. 3*C*, Q22; Fig. 3*E*, Q48) are soluble and normally confined in the cell cytoplasm, and testosterone-activated GFP-AR.Q0 (Fig. 3*B*) and GFP-AR.Q22 (Fig. 3*D*) are fully translocated into the nuclei. The testosterone-activated GFP-AR.Q48 may be detected in aggregates confined in the cell cytoplasm or in the cell processes (Fig. 3*F*). We have already reported that these inclusions are ubiquitinated (35) and that, in our experimental conditions, NSC34 cells do not contain nuclear aggregates. The correspondence of the AR immunofluorescence with the GFP-AR chimeras was confirmed with an anti-AR polyclonal antibody (AR-N20) (data not shown). The aggregates are found only after testosterone activation of the AR, probably because this treatment induces dissociation of the receptor from the chaperone proteins hsp90 and hsp70.

Examples of the different types of aggregates detectable in NSC34 cells are given in Fig. 4. On the basis of their size and cell localization, the aggregates have been classified as small cytoplasmic aggregates (diameter of about 0.5-2 μm; Fig. 4*A*), large cytoplasmic aggregates (diameter of about 3-10 μm; Fig. 4*B*), and neuropil aggregates (Fig. 4*C*, *D*; always classified as small). Small aggregates were generally diffusely localized throughout the cytoplasm, and large aggregates were generally confined to the perinuclear region of the immortalized motoneurons. The number of aggregates per cell was extremely variable, ranging from a single aggregate per cell (usually a large one) up to 30-40 per cell (in this case the aggregates were small).

Table 1 illustrates, for two times of observation, the total number of living immortalized motoneuronal cells displaying cytoplasmic or neuropil aggregates or both types of aggregates, as measured by fluorescence microscopic evaluation of the percentage of cells bearing a specific type of aggregate. The rate of aggregation in neurites is very low when compared with that found in the cytoplasm, and consequently, only a very limited number of cells is potentially sensitive (in this limited time window of observation) to alteration of the neuronal processes; this result is compatible with the long time required for symptoms to appear in all polyGln-related diseases.

Alteration of axonal trafficking

To evaluate possible alterations in the distribution of organelles in the neurites as a consequence of the presence of neuropil aggregates, NSC34 cells were cotransfected with both the GFP-AR.Q(n)s chimeras and mtBFP. The results obtained with living cells are shown in Fig. 5, in which we focused our attention on the cell processes, whereas the high-resolution images of the soma of NSC34 cells bearing neuropil aggregates are shown in Fig. 6. We analyzed several neurites of NSC34 cells transfected with the GFP-AR.Q(n)/mtBFP chimeras. At least two different phenotypes were observed in cells bearing neuropil inclusions. Figure 5 shows the appearance of representative NSC34 cells cotransfected with control GFP-AR.Q0 and mtBFP (Fig. 5*A*, *B*) or GFP-AR.Q22 and mtBFP (Fig. 5*C*, *D*) after testosterone treatment. AR proteins (Q0 or Q22) are confined to the nuclei, whereas mitochondria are distributed in the cell cytoplasm and along cell processes (obviously, the intensity of fluorescence in the neurites was considerably lower than that observed in the cytoplasm; therefore, this latter region appears moderately saturated in all images shown). However, in NSC34 cells expressing GFP-AR.Q48 and mtBFP, accumulation of mitochondria in the cell processes was detectable in close association to neuropil aggregates. In Fig. 5*E*, *F*, the NSC34/GFP-AR.Q48/mtBFP cell body adhered well to the coverslip, and it appears that mitochondria (in blue) are closely associated with two small aggregates (in green). This cell (Fig. 5*F*) exhibits a neurite of an unexpectedly large and constant diameter, with a substantially normal phenotype. Figure 5*G*, *H* depicts a representative NSC34/GFP-AR.Q48/mtBFP cell with an aberrant neurite morphology related to neuropil aggregates. In this case, as shown by the merged analysis (Fig. 5*H*), the accumulation of insoluble proteinaceous material (in green) resulted in three abnormal enlargements of the neurite caliber; these are accompanied by an increased number of organelles, e.g., mitochondria (in blue), in the swollen portions. It must be noted that the fiber depicted in Fig. 5*H* has a smaller diameter than the fiber shown in Fig. 5*F*. It is not possible, at the moment, to determine whether the smaller size is a result of neuropil inclusions present at the root of the fiber, which would possibly deprive the downstream compartment of material coming from the soma, or whether the small caliber per se may promote accumulation. Figure 5*I*, *J* shows a different NSC34/GFP-AR.Q48/mtBFP cell phenotype; in this case the neurite swelling is similar to that depicted in Fig. 5*H* but is apparently induced by the intersection of two processes arising from different cells (higher magnification of this intersection is shown in Fig. 5*K*). This suggests that the pressure exerted by one cell process on the other one may squeeze the neurite, causing total obstruction by the aggregate and consequently an accumulation of mitochondria. Axonal swelling may thus be secondary to the formation of inclusions in neurites.

To analyze whether aberrant distribution of mitochondria was also present in the cell cytoplasm (possibly because of an energy need for the formation of aggregates, or because of an early apoptotic process inducing mitochondria clustering), we used high-resolution fluorescence microscopy and focused our attention on the cell soma (unfortunately, because of the low intensity of fluorescence in the cell processes, in these conditions we were unable to obtain images of neurites in GFP-AR.Q0-transfected cells, whereas the mitochondria accumulation made it possible in GFP-AR.Q48/NSC34 cells bearing aggregates in the cell processes). It appears from Fig. 6 that in immortalized motoneuronal cells transfected with the chimera of with GFP-AR.Q0 (Fig. 6*A-C*), the AR protein is normally concentrated in the nuclei (Fig. 6*A*), whereas the mitochondria are well distributed in the cell cytoplasm (Fig. 6*B*). The different compartmentalization is evident in the merged analysis (Fig. 6*C*). Immortalized motoneuronal cells transfected with AR containing an elongated polyGln tract show aggregates localized in the cell cytoplasm and in cell processes (Fig. 6*D*). The distribution of mitochondria, labeled with mtBFP, is clearly altered in neuronal processes (Fig. 6*E*); the merged analysis (Fig. 6*F*) shows that mitochondria are detectable in large amounts in association with neuropil inclusions (Fig. 6*F*, marked with arrows; this is more evident at higher magnification in the inset), but not with cytoplasmic inclusions, suggesting that this effect is specific for the neuropil.

To evaluate the potential neurotoxicity of neuropil aggregates of GFP-AR.Q48 induced by testosterone treatment in transfected motoneuronal cells, we also analyzed whether fast axonal transport could be impaired by the inclusion. Because mitochondria are rapidly transported on microtubules through the axons by the motor protein kinesin, we analyzed the distribution of kinesin in cells bearing neuropil aggregates.

Figure 7 shows confocal microscopic images of fixed NSC34/GFP-AR.Q(n)s cells processed by using an anti-kinesin monoclonal antibody (MAB1614, Chemicon) and a TRICT-labeled secondary antybody. The analysis of kinesin distribution (in red) in NSC34 cells expressing the control GFP-AR.Q0 (Fig. 7*A*, in green) and the GFP-AR.Q22 (Fig. 7*C*, in green) shows that this motor protein is detectable in the whole cell, with homogeneous distribution along the cell processes. Figure 7B**,** *D* shows the same cells at light-transmitted microscopy. The distribution of kinesin in cells bearing neuropil aggregates is depicted in Fig. 7*E*, which shows the kinesin immunoreactivity in two contiguous cells (as shown by light microscopy in Fig. 7*H*). Figure 7*F* shows that both NSC34 cells were positive for GFP-AR.Q48, with a large amount of AR protein in the two cell nuclei, but only the upper cell contained neuropil aggregates. Figure 7*G* shows that kinesin was normally distributed in the lower cell devoid of neuropil aggregates, but the presence of inclusions in the processes (upper cell) heavily altered the kinesin distribution in the neurites, inducing a concentration of the motor protein in structures that resembled those observed in the case of the mitochondrial study. It must also be noted that the cell devoid of intracellular aggregates had normal kinesin distribution in the soma, whereas the cell containing several neuropil aggregates showed not only a large kinesin accumulation closely associated with the inclusions but also a loss of immunoreactive kinesin from the cell body (Figure 7*G*). At higher magnification, the same cell processes are evident in double fluorescence (Fig. 7*I*), and the two parallel neurites from distinct NSC34 cells are shown by light-transmitted microscopy (Fig. 7*J*). It is also possible to identify the location of the aggregates (merged analysis in Fig. 7*K*) within the upper neurite; little distortion of the axonal caliber was observed (Fig. 7*J*).

Occasionally, axonal swelling, containing a high proportion of immunoreactive kinesin, was also detectable in this fixed cell.

DISCUSSION

In the present paper, we analyzed the possible neurotoxicity of SBMA AR aggregates located in neuronal processes. In particular, we studied whether events mediated by the process of fast axonal transport sustained by kinesin can be modified by the presence of the aggregate inclusions in neurites, which would alter the bioavailability of important components for synaptic functions. To this purpose, we initially evaluated the rate of neuropil aggregate formation in immortalized motoneuronal cells (NSC34) transfected with SBMA AR, and we found that both types of cytoplasmic inclusions (perinuclear and neuropil) appeared only under the influence of androgens. In the absence of the hormone, the unliganded AR, which is normally entrapped in a multi-heteromeric inactive complex with accessory chaperone proteins (hsp90, hsp70), is probably protected from polyGln-induced aggregation. The chaperones either may mask the polyGln tract, which would counteract its natural tendency to cross-link with other polyGlns (54-56), or may repair the misfolding induced by the expanded polyGln of the mutant AR protein (57). Testosterone, by inducing dissociation of AR from chaperones, allows the mutated protein to acquire the misfolded conformation responsible for initiation of the aggregation process (40, 45).

It is not clear, however, whether neuropil aggregates derive from cytoplasmic aggregates migrated into the cone of the processes, or whether they are directly formed in the neurites. The fact that GFP-AR.Q48 chimeric protein is detectable in the neurites in the absence of testosterone, when aggregates are not yet present, suggests that these inclusions may originate directly in the cell processes after androgenic treatment. This suggestion is supported by the observations that neuropil aggregates are also detectable in cells not showing cytoplasmic aggregates and that neuropil inclusions appear in a relatively low number of transfected cells (about 10-15% of total transfected immortalized motoneuronal cells); consequently, the potential toxicity of these inclusions cannot be measured with standard cell viability tests (35). However, this low number of inclusions in the cell processes may explain why, up to now, they have not been observed in SBMA transgenic mice (58).

Neuropil aggregates have been reported in vivo in another well-studied polyGln-related disease HD: in the brains of HD patients (39), as well as in the corresponding transgenic mice (24), these aggregates are highly concentrated in the axons of striatal neurons, the first cells that degenerate in HD, whereas intranuclear inclusions are mainly present in cortical neurons, which are affected at later stages of the disease. Moreover, the total number of neuropil aggregates found in vivo in the juvenile form of HD (a more aggressive form of HD caused by extremely long polyGln expansions) is higher than that observed in late-onset form of the disease (in which the size of the polyGln expansion is just above the threshold value of 40). These observations suggest a direct role of neuropil aggregates in the neurodegeneration of HD.

To evaluate possible alterations of the transport through the cell processes, we studied the distribution of mitochondria in cell processes after cotransfection of immortalized motoneuronal cells (NSC34) with GFP-tagged wild-type or mutated ARs, and mtBFP. The combined use of the

two fluorescent proteins, with distinct spectral and targeting properties, allowed the simultaneous identification of AR aggregation and of mitochondrial distribution in living immortalized motoneuronal cells. After testosterone induction of AR aggregates, we observed wild-type AR protein normally concentrated into the nuclei and the mitochondria well distributed in the cell cytoplasm. In contrast, the distribution of mitochondria was clearly altered in neuronal processes of immortalized motoneuronal cells transfected with AR bearing the expanded polyGln tract and containing neuropil aggregates: mitochondria accumulated along the processes close to the aggregate (either upstream or downstream), possibly because aggregates physically alter neurite trafficking. Mitochondria may also become aberrantly distributed because of an increased energy need in the vicinity of the aggregate; however, no sequestering of mitochondria by aggregates was observed in the cell cytoplasm. Of particular relevance is that, in our motoneuronal cell system, the neuropil aggregates were occasionally accompanied by neurite swellings rich in mitochondria. The swelling of cell processes with mitochondrial accumulation can also be seen in vitro at the intersection of two cell processes. Transposed into an in vivo situation, this result suggests that the primary event in neuropil aggregate accumulation, and consequently in the alteration of mitochondrial transport, may be generated not only by variations in nerve caliber at particular districts (such as at the nodes of Ranvier) but also by nerve compression. Interestingly, the same type of neurite swelling has been described in other neurodegenerative disorders (such as amyotrophic lateral sclerosis [ALS]) (59).

Mitochondria are actively transported through the axons via a microtubule-based system that utilizes specific motor proteins of the kinesin and dynein families, which transport several different neuronal cargoes. These proteins exert their action along the neuronal processes themselves or at the synapses. Damage to this highly controlled axonal transport may result in axonal malfunction, axonal loss, and consequently motoneuronal cell death (60). In particular, mitochondria are specifically transported both by classic kinesin (61) and by another member of the kinesin superfamily, KIF 1B (62). Confocal microscopic analysis allowed identification of regions upstream of neuropil aggregates in which the levels of kinesin were much higher than those normally found in cells processes devoid of aggregates; the accumulation of kinesin was occasionally associated with swellings (not shown). Therefore, accumulation of proteinaceous material in the processes of motoneuronal cells may result in a slow depletion of important components required for axonal functions or may induce axonal strangulation; both processes may then lead to neuronal dysfunction followed by axonal degeneration, which would then affect the soma and induce cell death.

Our study provides the first experimental evidence that in polyGln-related disorders, intraneuronal aggregates in the cell processes may profoundly alter the process of fast axonal transport by blocking one of the major effectors, the motor protein kinesin. Interestingly, in *Drosophila melanogaster*, mutants lacking the kinesin heavy chain are lethal and exhibit an alteration in the motoneuronal phenotype, accompanied by accumulation of material in “clogs” along axons, that disrupts neuronal functions (63). Moreover, as reported in Kennedy’s disease (64) and in a transgenic mouse model for familial ALS, neurofilament-rich inclusions are present in axons, and these inclusions reduce the transport of selective cargoes (65, 66). Axonal swellings and spheroids have also been reported in the spinal cord of patients with motoneuron disease (67). Finally, depletion of sensory neurons in the dorsal root ganglia is detectable in SBMA (recently reclassified as a neuropathy) (5, 64, 68, 69). It is of note that defects in axonal

transport, induced by a mutation in the motor protein KIF1Bβ, is responsible for axonopathy in the inherited human neuropathy Charcot-Marie-Tooth disease type 2A (70). On the basis of our results, a similar mechanism may be hypothesized for SBMA.

Alterations of axonal functions in SBMA and possibly in other polyGln-related disorders may represent one of the multifactorial events capable of inducing cell death (17, 21, 35, 40, 42, 44, 71-78). The multistep neurodegenerative process also includes the toxicity mediated by intranuclear inclusions (25, 26) (but not that of cytoplasmic perinuclear inclusions; see ref 35), which may sequester CREB-binding protein, an essential transcriptional coactivator, leading to altered control of gene expression in motoneuronal cells of SBMA patients.

Neuropil inclusions may thus become toxic and act as a second (or third and final?) step in the neurodegenerative process, and it is conceivable that these occlusions occurring in axons may lead to the formation of the dystrophic neurites (20, 24, 35, 36, 39, 40, 79). It is therefore evident that the processes involved in the formation of cytoplasmic, neuropil, and nuclear inclusions (and their neurotoxicity) are rather different and that the three types of aggregates may play different roles in the multistep events required for the pathogenesis of SBMA.

ACKNOWLEDGMENTS

The financial support of Telethon-Italy (grants 1283, 1285, GTF01011, and GP0222/01) is gratefully acknowledged. This work was also supported in part by the Italian Ministry of University and Research (MIUR), FIRB (grant RBAU01NXFP), the Italian Ministry of Health RF93-2002, the Italian Association for Cancer Research (AIRC), Italian National Research Council (CNR), the Human Frontier Science Program, and the Italian Space Agency (ASI). The authors wish to thank Dr. Neil R. Cashman for providing the NSC34 cells.

REFERENCES

1. Cummings, C.J., Zoghbi, H.Y. (2000) Fourteen and counting: unraveling trinucleotide repeat diseases. *Hum Mol Genet* **9,** 909-916

2. Nakamura, K., Jeong, S.Y., Uchihara, T., Anno, M., Nagashima, K., Nagashima, T., Ikeda, S., Tsuji, S., Kanazawa, I. (2001) SCA17, a novel autosomal dominant cerebellar ataxia caused by an expanded polyglutamine in TATA-binding protein. *Hum Mol Genet* **10,** 1441-1448

3. La Spada, A.R., Wilson, E.M., Lubahn, D.B., Harding, A.E., Fischbeck, K.H. (1991) Androgen receptor gene mutations in X-linked spinal and bulbar muscular atrophy. *Nature (London)* **352,** 77-79

4. Kennedy, W.R., Alter, M., Sung, J.H. (1968) Progressive proximal spinal and bulbar muscular atrophy of late onset. A sex-linked recessive trait. *Neurology* **18,** 671-680

5. Sobue, G., Hashizume, Y., Mukai, E., Hirayama, M., Mitsuma, T., Takahashi, A. (1989) X-linked recessive bulbospinal neuronopathy. A clinicopathological study. *Brain* **112,** 209-232

6. Andrew, S.E., Goldberg, Y.P., Hayden, M.R. (1997) Rethinking genotype and phenotype correlations in polyglutamine expansion disorders. *Hum Mol Genet* **6,** 2005-2010

7. Ikonen, T., Palvimo, J.J., Janne, O.A. (1997) Interaction between the amino- and carboxyl-terminal regions of the rat androgen receptor modulates transcriptional activity and is influenced by nuclear receptor coactivators. *J Biol Chem* **272,** 29821-29828

8. La Spada, A.R., Roling, D.B., Harding, A.E. (1992) Meiotic stability and genotype correlation of the trinucleotide repeat in X-linked spinal and bulbar muscular atrophy. *Nat Genet* **2,** 301-304

9. Morrison, P.J., Mirakhur, M., Patterson, V. (1998) Discordant repeat size and phenotype in Kennedy syndrome. *Clin Genet* **53,** 276-277

10. Chamberlain, N.L., Driver, E.D., Miesfeld, R.L. (1994) The length and location of CAG trinucleotide repeats in the androgen receptor N-terminal domain affect transactivation function. *Nucleic Acids Res* **22,** 3181-3186

11. Choong, C.S., Wilson, E.M. (1998) Trinucleotide repeats in the human androgen receptor: a molecular basis for disease. *J Mol Endocrinol* **21,** 235-257

12. Gao, T., Marcelli, M., McPhaul, M.J. (1996) Transcriptional activation and transient expression of the human androgen receptor. *J Steroid Biochem Mol Biol* **5,** 9-20

13. Kazemi-Esfarjani, P., Trifiro, M.A., Pinsky, L. (1995) Evidence for a repressive function of the long polyglutamine tract in the human androgen receptor: possible pathogenetic relevance for the $(CAG)_n$-expanded neuronopathies. *Hum Mol Genet* **4,** 523-527

14. Mhatre, A.N., Trifiro, M.A., Kaufman, M., Kazemi-Esfarjani, P., Figlewicz, D., Rouleau, G., Pinsky, L. (1993) Reduced transcriptional regulatory competence of the androgen receptor in X-linked spinal and bulbar muscular atrophy. *Nat Genet* **5,** 184-188

15. Abdullah, A.A.R., Trifiro, M.A., Panetraymond, V., Alvarado, C., Detourreil, S., Frankel, D., Schipper, H.M., Pinsky, L. (1998) Spinobulbar muscular atrophy-polyglutamine-expanded androgen receptor is proteolytically resistant in vitro and processed abnormally in transfected cells. *Hum Mol Genet* **7,** 379-384

16. Brooks, B.P., Paulson, H.L., Merry, D.E., Salazar-Grueso, E.F., Brinkmann, A.O., Wilson, E.M., Fischbeck, K.H. (1997) Characterization of an expanded glutamine repeat androgen receptor in a neuronal cell culture system. *Neurobiol Dis* **3,** 313-323

17. Butler, R., Leigh, P.N., McPhaul, M.J., Gallo, J.M. (1998) Truncated forms of the androgen receptor are associated with polyglutamine expansion in X-linked spinal and bulbar muscular atrophy. *Hum Mol Genet* **7,** 121-127

18. Davies, S.W., Turmaine, M., Cozens, B.A., DiFiglia, M., Sharp, A.H., Ross, C.A., Scherzinger, E., Wanker, E.E., Mangiarini, L., Bates, G.P. (1997) Formation of neuronal intranuclear inclusions underlies the neurological dysfunction in mice transgenic for the HD mutation. *Cell* **90,** 537-548

19. Davies, S.W., Beardsall, K., Turmaine, M., DiFiglia, M., Aronin, N., Bates, G.P. (1998) Are neuronal intranuclear inclusions the common neuropathology of triplet-repeat disorders with polyglutamine-repeat expansions? *Lancet* **351,** 131-133

20. DiFiglia, M., Sapp, E., Chase, K.O., Davies, S.W., Bates, G.P., Vonsattel, J.P., Aronin, N. (1997) Aggregation of huntingtin in neuronal intranuclear inclusions and dystrophic neurites in brain. *Science* **277,** 1990-1993

21. Ellerby, L.M., Hackam, A.S., Propp, S.S., Ellerby, H.M., Rabizadeh, S., Cashman, N.R., Trifiro, M.A., Pinsky, L., Wellington, C.L., Salvesen, G.S., Hayden, M.R., Bredesen, D.E. (1999) Kennedy's disease: caspase cleavage of the androgen receptor is a crucial event in cytotoxicity. *J Neurochem* **72,** 185-195

22. Igarashi, S., Koide, R., Shimohata, T., Yamada, M., Hayashi, Y., Takano, H., Date, H., Oyake, M., Sato, T., Sato, A., Egawa, S., Ikeuchi, T., Tanaka, H., Nakano, R., Tanaka, K., Hozumi, I., Inuzuka, T., Takahashi, H., Tsuji, S. (1998) Suppression of aggregate formation and apoptosis by transglutaminase inhibitors in cells expressing truncated DRPLA protein with an expanded polyglutamine stretch. *Nat Genet* **18,** 111-117

23. Jones, A.L., Wood, J.D., Harper, P.S. (1997) Huntington disease: advances in molecular and cell biology. *J Inherit Metab Dis* **20,** 125-138

24. Li, H., Li, S.-H., Cheng, A.L., Mangiarini, L., Bates, G.P., Li, X.-J. (1999) Ultrastructural localization and progressive formation of neuropil aggregates in Huntington's disease transgenic mice. *Hum Mol Genet* **8,** 1227-1236

25. Li, M., Miwa, S., Kobayashi, Y., Merry, D., Yamamoto, M., Tanaka, F., Doyu, M., Hashizume, Y., Fischbeck, K.H., Sobue, G. (1998) Nuclear inclusions of the androgen receptor protein in spinal and bulbar muscular atrophy. *Ann Neurol* **44,** 249-254

26. Li, M., Nakagomi, Y., Kobayashi, Y., Merry, D., Tanaka, F., Doyu, M., Mitsuma, T., Hashizume, Y., Fischbeck, K.H., Sobue, G. (1998) Nonneural nuclear inclusions of androgen receptor protein in spinal and bulbar muscular atrophy. *Am J Pathol* **153,** 695-701

27. Lieberman, A.P., Robitaille, Y., Trojanowski, J.Q., Dickson, D.W., Fischbeck, K.H. (1998) Polyglutamine-containing aggregates in neuronal intranuclear inclusion disease. *Lancet* **351,** 884

28. Martindale, D., Hackam, A., Wieczorek, A., Ellerby, L., Wellington, C., McCutcheon, K., Singaraja, R., Kazemi-Esfarjani, P., Devon, R., Kim, S.U., Bredesen, D.E., Tufaro, F., Hayden, M.R. (1998) Length of huntingtin and its polyglutamine tract influences localization and frequency of intracellular aggregates. *Nat Genet* **18,** 150-154

29. Moulder, K.L., Onodera, O., Burke, J.R., Strittmatter, W.J., Johnson, E.M.J. (1999) Generation of neuronal intranuclear inclusions by polyglutamine-GFP: analysis of inclusion clearance and toxicity as a function of polyglutamine length. *J Neurosci* **19,** 705-715

30. Onodera, O., Burke, J.R., Miller, S.E., Hester, S., Tsuji, S., Roses, A.D., Strittmatter, W.J. (1997) Oligomerization of expanded-polyglutamine domain fluorescent fusion proteins in cultured mammalian cells. *Biochem Biophys Res Commun* **238,** 599-605

31. Ordway, J.M., Tallaksen-Greene, S., Gutekunst, C.A., Bernstein, E.M., Cearley, J.A., Wiener, H.W., Dure, L.S., Lindsey, R., Hersch, S.M., Jope, R.S., Albin, R.L., Detloff, P.J. (1997) Ectopically expressed CAG repeats cause intranuclear inclusions and a progressive late onset neurological phenotype in the mouse. *Cell* **91,** 753-763

32. Paulson, H.L., Das, S.S., Crino, P.B., Perez, M.K., Patel, S.C., Gotsdiner, D., Fischbeck, K.H., Pittman, R.N. (1997) Machado-Joseph disease gene product is a cytoplasmic protein widely expressed in brain. *Ann Neurol* **41,** 453-462

33. Paulson, H.L., Perez, M.K., Trottier, Y., Trojanowski, J.Q., Subramony, S.H., Das, S.S., Vig, P., Mandel, J.L., Fischbeck, K.H., Pittman, R.N. (1997) Intranuclear inclusions of expanded polyglutamine protein in spinocerebellar ataxia type 3. *Neuron* **19,** 333-344

34. Scherzinger, E., Lurz, R., Turmaine, M., Mangiarini, L., Hollenbach, B., Hasenbank, R., Bates, G.P., Davies, S.W., Lehrach, H., Wanker, E.E. (1997) Huntingtin-encoded polyglutamine expansions form amyloid-like protein aggregates in vitro and in vivo. *Cell* **90,** 549-558

35. Simeoni, S., Mancini, M.A., Stenoien, D.L., Marcelli, M., Weigel, N.L., Zanisi, M., Martini, L., Poletti, A. (2000) Motoneuronal death does not correlate with aggregate formation in spinobulbar muscular atrophy. *Hum Mol Genet* **9,** 133-144

36. Singhrao, S.K., Thomas, P., Wood, J.D., MacMillan, J.C., Neal, J.W., Harper, P.S., Jones, A.L. (1998) Huntingtin protein colocalizes with lesions of neurodegenerative diseases: an investigation in Huntington's, Alzheimer's, and Pick's diseases. *Exp Neurol* **150,** 213-222

37. Stenoien, D.L., Cummings, C.J., Adams, H.P., Mancini, M.G., Patel, K., DeMartino, G., Marcelli, M., Weigel, N.L., Mancini, M.A. (1999) Polyglutamine-expanded androgen

receptors form aggregates that sequester heat shock proteins, proteasome components and SRC-1, and are suppressed by the HDJ-2 chaperone. *Hum Mol Genet* **8,** 731-741

38. Yagishita, S., Inoue, M. (1997) Clinicopathology of spinocerebellar degeneration: its correlation to the unstable CAG repeat of the affected gene. *Pathol Int* **47,** 1-15

39. Gutekunst, C.A., Li, S.H., Yi, H., Mulroy, J.S., Kuemmerle, S., Jones, R., Rye, D., Ferrante, R.J., Hersch, S.M., Li, X.J. (1999) Nuclear and neuropil aggregates in Huntington's disease: relationship to neuropathology. *J Neurosci* **19,** 2522-2534

40. Piccioni, F., Simeoni, S., Andriola, I., Armatura, E., Bassanini, S., Pozzi, P., Martini, L., Poletti, A. (2001) Polyglutamine tract expansion in the androgen receptor in a motoneuronal model of spinal and bulbar muscular atrophy. *Brain Res Bull* **56,** 215-220

41. Poletti, A. (1999) CAG expansion in androgen receptor gene and neuronal cell death. *Recent Res Dev Neurochem* **2,** 507-515

42. Saudou, F., Finkbeiner, S., Devys, D., Greenberg, M.E. (1998) Huntingtin acts in the nucleus to induce apoptosis but death does not correlate with the formation of intranuclear inclusions. *Cell* **95,** 55-66

43. Sisodia, S.S. (1998) Nuclear inclusions in glutamine repeat disorders---are they pernicious, coincidental, or beneficial? *Cell* **95,** 1-4

44. Merry, D.E., Kobayashi, Y., Bailey, C.K., Taye, A.A., Fischbeck, K.H. (1998) Cleavage, aggregation and toxicity of the expanded androgen receptor in spinal and bulbar muscular atrophy. *Hum Mol Genet* **7,** 693-701

45. Kobayashi, Y., Kume, A., Li, M., Doyu, M., Hata, M., Ohtsuka, K., Sobue, G. (2000) Chaperones Hsp70 and Hsp40 suppress aggregate formation and apoptosis in cultured neuronal cells expressing truncated androgen receptor protein with expanded polyglutamine tract. *J Biol Chem* **275,** 8772-8778

46. McCampbell, A., Taylor, J.P., Taye, A.A., Robitschek, J., Li, M., Walcott, J., Merry, D., Chai, Y., Paulson, H., Sobue, G., Fischbeck, K.H. (2000) CREB-binding protein sequestration by expanded polyglutamine. *Hum Mol Genet* **9,** 2197-2202

47. Nagai, Y., Onodera, O., Strittmatter, W.J., Burke, J.R. (1999) Polyglutamine domain proteins with expanded repeats bind neurofilament, altering the neurofilament network. *Ann N Y Acad Sci* **893,** 192-202

48. Poletti, A., Negri-Cesi, P., Rabuffetti, M., Colciago, A., Celotti, F., Martini, L. (1998) Transient expression of the type 2 5α-reductase isozyme in the brain of the late fetal and early post-natal life. *Endocrinology* **139,** 2171-2178

49. Rizzuto, R., Pinton, P., Carrington, W., Fay, F.S., Fogarty, K.E., Lifshitz, L.M., Tuft, R.A., Pozzan, T. (1998) Close contacts with the endoplasmic reticulum as determinants of mitochondrial Ca^{2+} responses. *Science* **280,** 1763-1766

50. Cashman, N.R., Durham, H.D., Blusztajn, J.K., Oda, K., Tabira, T., Shaw, I.T., Dahrouge, S., Antel, J.P. (1992) Neuroblastoma × spinal cord (NSC) hybrid cell lines resemble developing motor neurons. *Dev Dyn* **194,** 209-221

51. Durham, H.D., Dahrouge, S., Cashman, N.R. (1992) Evaluation of the spinal cord neuron × neuroblastoma hybrid cell line NSC-34 as a model for neurotoxicity testing. *Neurotoxicology* **14,** 387-395

52. Poletti, A., Rampoldi, A., Piccioni, F., Ponti, N., Simeoni, S., Volpi, S., Zanisi, M., Martini, L. (2001) 5α-Reductase type 2 and androgen receptor compose the androgen responsiveness of the gonadotropin-releasing hormone (GnRH) GT1-1 neurons**.** *J Neuroendocrinol* **13,** 353-357

53. Zhou, Z.X., Lane, M.V., Kemppainen, J.A., French, F.S., Wilson, E.M. (1995) Specificity of ligand-dependent androgen receptor stabilization: receptor domain interactions influence ligand dissociation and receptor. *Mol Endocrinol* **9,** 208-218

54. Perutz, M.F. (1994) Polar zippers: their role in human disease. *Protein Sci* **3,** 1629-1637

55. Perutz, M.F., Johnson, T., Suzuki, M., Finch, J.T. (1994) Glutamine repeats as polar zippers: their possible role in inherited neurodegenerative diseases. *Proc Natl Acad Sci USA* **91,** 5355-5358

56. Altschuler, E.L., Hud, N.V., Mazrimas, J.A., Rupp, B. (1997) Random coil conformation for extended polyglutamine stretches in aqueous soluble monomeric peptides. *J Pept Res* **50,** 73-75

57. Paulson, H.L. (1999) Protein fate in neurodegenerative proteinopathies: polyglutamine diseases join the (mis)fold. *Am J Hum Genet* **64,** 339-345

58. Adachi, H., Kume, A., Li, M., Nakagomi, Y., Niwa, H., Do, J., Sang, C., Kobayashi, Y., Doyu, M., Sobue, M. (2001) Transgenic mice with an expanded CAG repeat controlled by the human AR promoter show polyglutamine nuclear inclusions and neuronal dysfunction without neuronal cell death. *Hum Mol Genet* **10,** 1039-1048

59. Harry, G.J. (1992) Acrylamide-induced alterations in axonal transport. Biochemical and autoradiographic studies. *Mol Neurobiol* **6,** 203-216

60. Goldstein, L.S., Yang, Z. (2000) Microtubule-based transport systems in neurons: the roles of kinesins and dyneins. *Annu Rev Neurosci* **23,** 39-71

61. Nobutaka, H. (1998) Kinesin and dynein superfamily proteins and the mechanism of organelle transport. *Science* **279,** 519-526

62. Nangaku, M., Yoshitake, R.S., Okada, Y., Noda, Y., Takemura, R., Yamazaki, H., Hirokawa, N. (1994) KIF1B, a novel microtuble plus end-directed monomeric motor protein for transport of mitochondria. *Cell* **79,** 1209-1220

63. Hurd, D.D., Saxton, W.M. (1996) Kinesin mutations cause motor neuron disease phenotypes by disrupting fast axonal transport in *Drosophila*. *Genetics* **144,** 1075-1085

64. Gallo, J.-M. (2001) Kennedy's disease: a triplet repeat disorder or a motor neuron disease? *Brain Res Bull* **56,** 209-214

65. Zhang, B., Tu, P., Abtahian, F., Trojanowski, J.Q., Lee, V.M. (1997) Neurofilaments and orthograde transport are reduced in ventral root axons of transgenic mice that express human SOD1 with a G93A mutation. *J Cell Biol* **139,** 1307-1315

66. Williamson, T.L., Cleveland, D.W. (1999) Slowing of axonal transport is a very early event in the toxicity of ALS-linked SOD1 mutants to motor neurons. *Nat Neurosci* **2,** 50-56

67. Toyoshima, I., Sugawara, M., Kato, K., Wada, C., Hirota, K., Hasegawa, K., Kowa, H., Sheetz, M.P., Masamune, O. (1998) Kinesin and cytoplasmic dynein in spinal spheroids with motor neuron disease. *J Neurol Sci* **159,** 38-44

68. Fischbeck, K.H. (1997) Kennedy disease. *J Inherit Metab Dis* **20,** 152-158

69. Fischbeck, K.H. (2001) Polyglutamine expansion neurodegenerative disease. *Brain Res Bull* **56,** 161-163

70. Zhao, C., Takita, J., Tanaka, Y., Setou, M., Nakagawa, T., Takeda, S., Yang, H.W., Terada, S., Nakata, T., Takei, Y., Saito, M., Tsuji, S., Hayashi, Y., Hirokawa, N. (2001) Charcot-Marie-Tooth disease type 2A caused by mutation in a microtubule motor KIF1B. *Cell* **105,** 587-597

71. Cattaneo, E., Rigamonti, D., Goffredo, D., Zuccato, C., Squitieri, F., Sipione, S. (2001) Loss of normal huntingtin function: new developments in Huntington's disease. *Trends Neurosci* **24,** 182-188

72. Klement, I.A., Skinner, P.J., Kaytor, M.D., Yi, H., Hersch, S.M., Clark, H.B., Zoghbi, H.Y., Orr, H.T. (1998) Ataxin-1 nuclear localization and aggregation---role in polyglutamine-induced disease in SCA1 transgenic mice. *Cell* **95,** 41-53

73. Rigamonti, D., Sipione, S., Goffredo, D., Zuccato, C., Fossale, E., Cattaneo, E. (2001) Huntingtin's neuroprotective activity occurs via inhibition of procaspase-9 processing. *J Biol Chem* **276,** 14545-14548

74. Zuccato, C., Ciammola, A., Rigamonti, D., Leavitt, B.R., Goffredo, D., Conti, L., MacDonald, M.E., Friedlander, R.M., Silani, V., Hayden, M.R., Timmusk, T., Sipione, S., Cattaneo, E. (2001) Loss of Huntingtin-mediated BDNF gene transcription in Huntington's disease. *Science* **293,** 493-498

75. Merry, D.E. (2001) Molecular pathogenesis of spinal and bulbar muscular atrophy. *Brain Res Bull* **56,** 203-207

76. Hirakura, Y., Azimov, R., Azimova, R., Kagan, B.L. (2000) Polyglutamine-induced ion channels: a possible mechanism for the neurotoxicity of Huntington and other CAG repeat diseases. *J Neurosci Res* **60,** 490-494

77. Monoi, H., Futaki, S., Kugimiya, S., Minakata, H., Yoshihara, K. (2000) Poly-L-glutamine forms cation channels: relevance to the pathogenesis of the polyglutamine diseases. *Biophys J* **7,** 2892-2899

78. Sculptoreanu, A., Abramovici, H., Abdullah, A.A., Bibikova, A., Panet-Raymond, V., Frankel, D., Schipper, H.M., Pinsky, L., Trifiro, M.A. (2000) Increased T-type Ca^{2+} channel activity as a determinant of cellular toxicity in neuronal cell lines expressing polyglutamine-expanded human androgen receptors. *Mol Cell Biochem* **203,** 23-31

79. Cooper, J.K., Schilling, G., Peters, M.F., Herring, W.J., Sharp, A.H., Kaminsky, Z., Masone, J., Khan, F.A., Delanoy, M., Borchelt, D.R., Dawson, V.L., Dawson, T.M., Ross, C.A. (1998) Truncated N-terminal fragments of huntingtin with expanded glutamine repeats form nuclear and cytoplasmic aggregates in cell culture. *Hum Mol Genet* **7,** 783-790.

Received February 14, 2002; accepted May 29, 2002.

Table 1

Aggregate formation in immortalized motoneuronal cells expressing AR with an elongated polyGln tract

Observation time point [a]	% Cells with cytoplasmic aggregates only			% Cells with neuropil aggregates			% Cells without aggregates	% Cells with all aggregates
(*N* = 12)	Total	Small	Large	Total	Neuropil	Cytoplasmic and neuropil		
48 h	29.1 ± 8.44	7.51 ± 4.65	21.63 ± 4.87	6.22 ± 2.38	0.24 ± 0.39	5.97 ± 2.29	64.63 ± 10.00	35.36 ± 10.11
72 h	18.19 ± 4.14	3.9 ± 1.79	14.34 ± 3.46	5.90 ± 2.32	0.51 ± 0.45	5.38 ± 2.41	75.89 ± 5.46	24.10 ± 5.46

[a] *N* = 12 represents the number of wells counted (in six different discrete regions) for each time point of observation.

Fig. 1

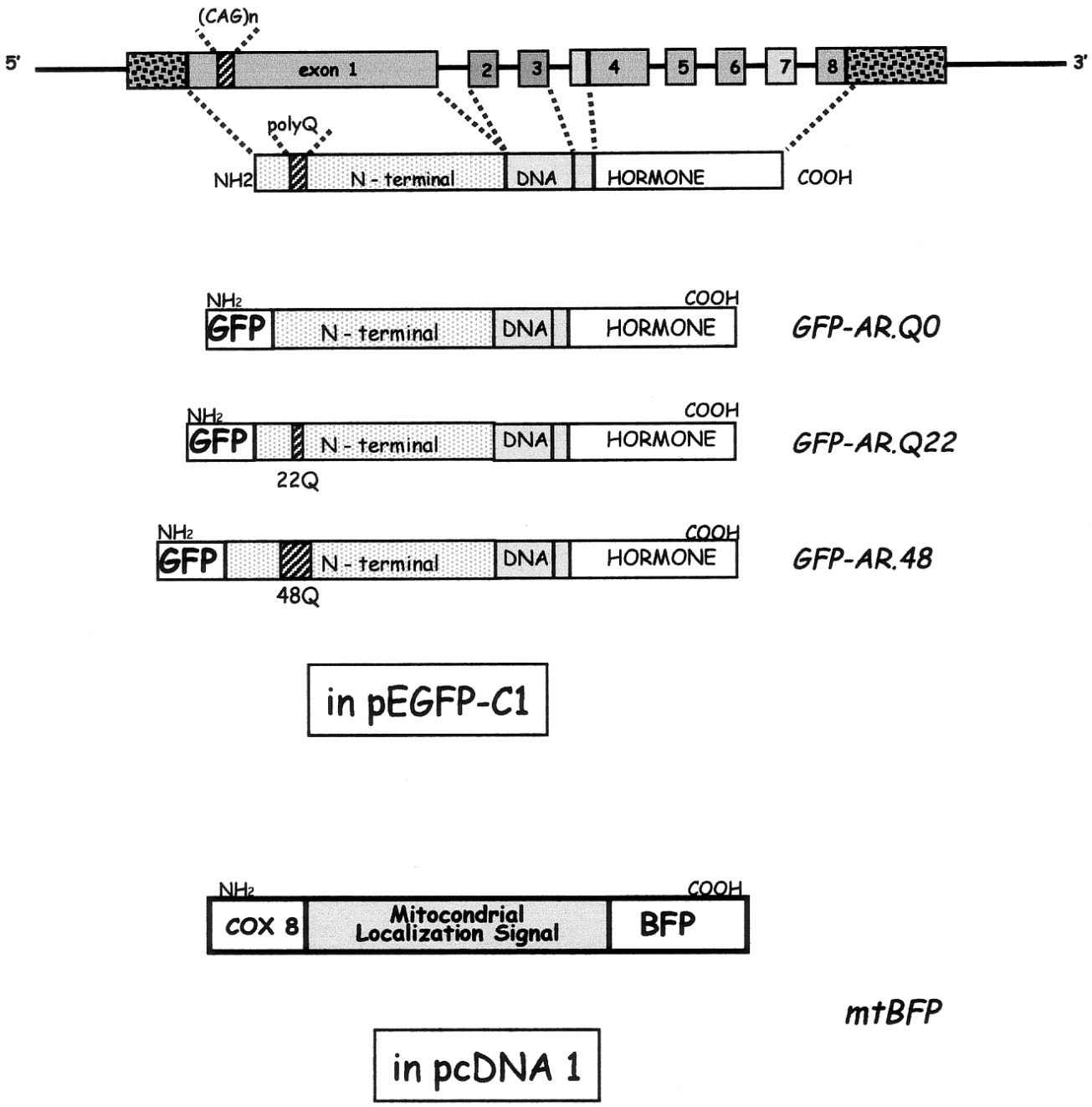

Figure 1. Schematic representation of the GFP or BFP chimeras utilized throughout the study: GFP-AR.Q0 indicates GFP-tagged AR in which the polyGln tract was artificially removed; GFP-AR.Q22 and GFP-AR.Q48 indicate GFP-tagged ARs in which the polyGln tracts were, respectively, composed of 22 (wild-type) or 48 (SBMA AR) contiguous glutamines. The cDNAs coding for the AR proteins have been cloned in pEGFP-C1. mtBFP indicates a BFP protein containing the mitochondrial localization signal of the COX8 gene.

Fig. 2

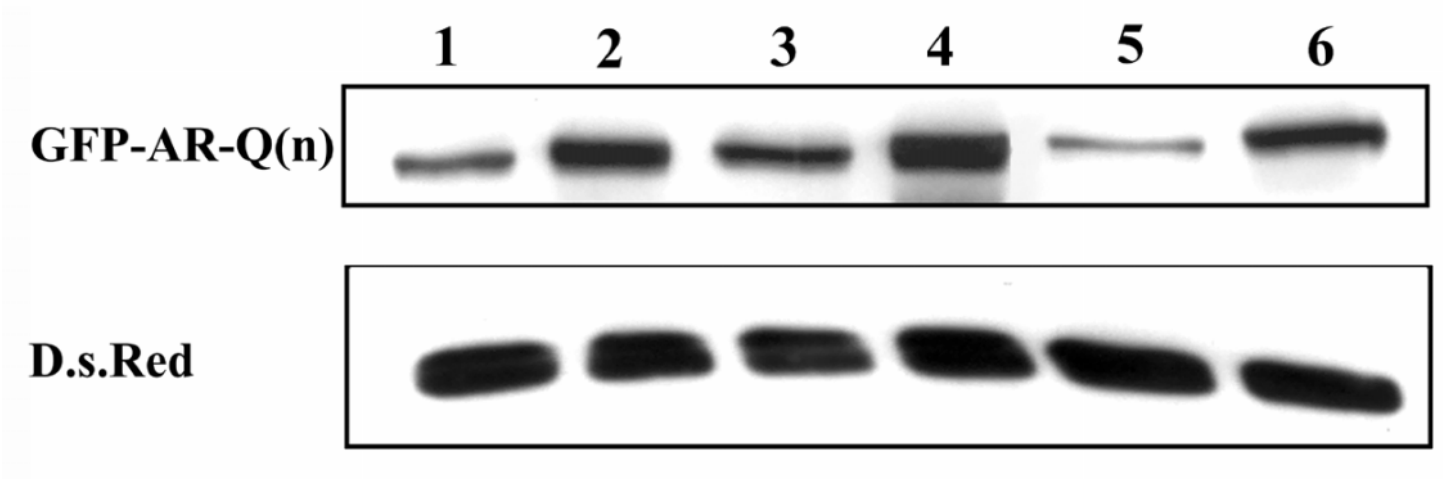

Figure 2. **Western blot analysis of NSC34 cells cotrasfected with GFP-AR.Q(n) chimeric constructs and pDSRed1-N1 plasmid (panel D.s.Red, the protein used to normalize transfection efficiency).** Immunoblot analysis was performed using the AR (N-20) polyclonal antibody to detect AR, and the D.s.Red antibody to detect fluorescent protein. Lanes 1 and 2 were loaded with samples obtained from NSC34/GFP-AR.Q0. Lanes 3 and 4 were loaded with samples obtained from NSC34/GFP-AR.Q22. Lanes 5 and 6 were loaded with samples obtained from NSC34/GFP-AR.Q48. Lanes 1, 3, and 5 were loaded with GFP-AR.Q(n)-transfected cells not exposed to testosterone, whereas lanes 2, 4, and 6 were loaded with GFP-AR.Q(n)-transfected cells treated with testosterone.

Fig. 3

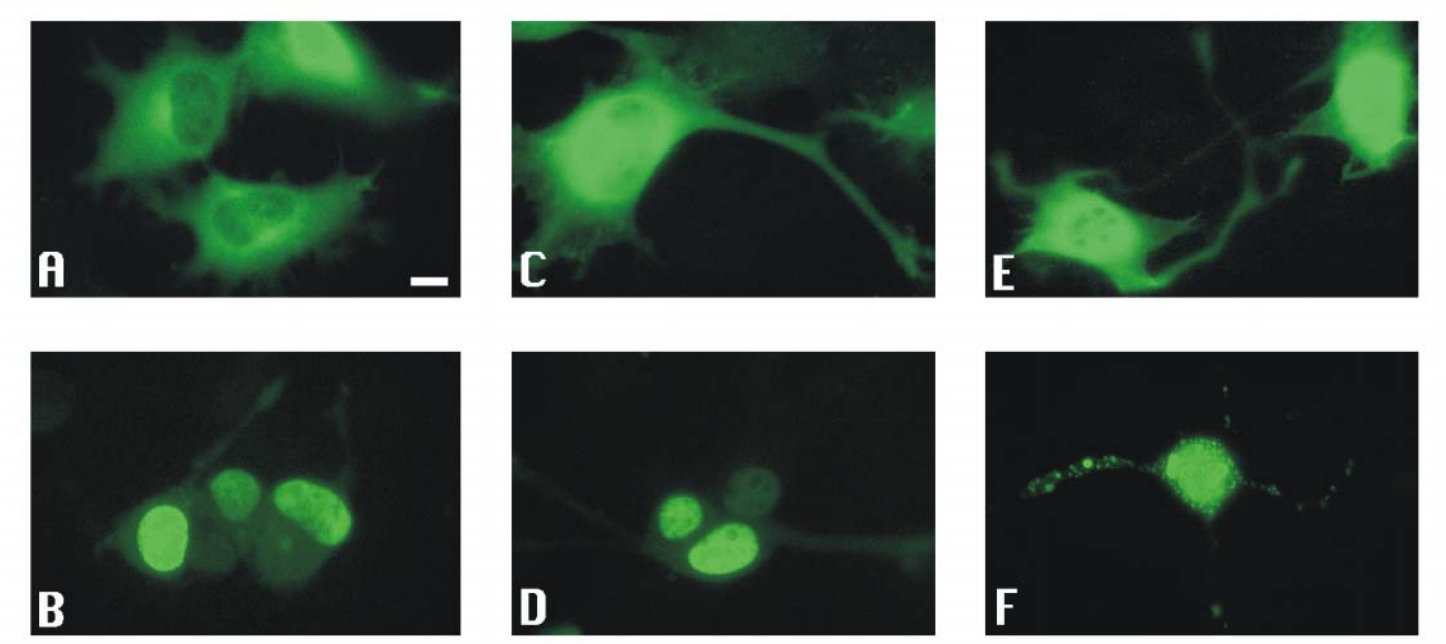

Figure 3. **Aggregate formation in NSC34 cells transiently transfected with GFP-AR.Q(n). A)** Control NSC34 cells expressing GFP-AR.Q0. **B)** NSC34 cells expressing GFP-AR.Q0 treated with testosterone. **C)** Control NSC34 cells expressing GFP-AR.Q22. **D)** NSC34 cells expressing GFP-AR.Q22 treated with testosterone. **E)** Control NSC34 cells expressing GFP-AR.Q48. **F)** NSC34 cells expressing GFP-AR.Q48 treated with testosterone. Scale bar = 10 µm.

Fig. 4

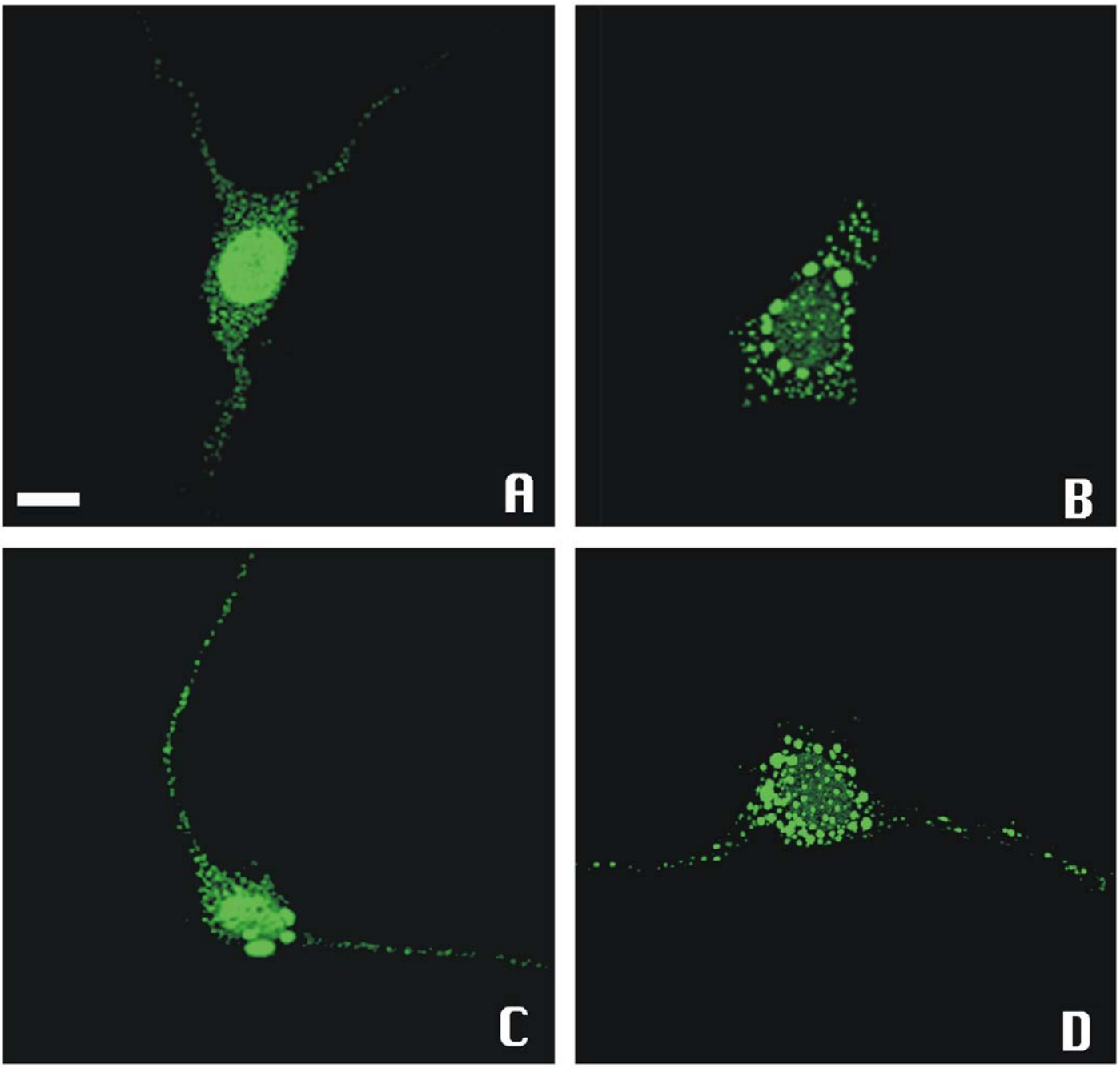

Figure 4. **Aggregate localization in NSC34 cells transiently transfected with GFP-AR.Q48.** NSC34 cells were transiently transfected with a plasmid expressing chimeras of GFP and the ARs bearing the elongated polyGln. The cells were treated with 1 µM testosterone for 48 h to induce the formation of aggregates. Living cells were observed with a fluorescence reverse-phase microscope using the FITC set of filters. **A)** Appearance of testsoterone-inducible small cytoplasmic perinuclear and neuropil aggregates of the GFP-AR.Q48 chimera. **B)** Distribution of perinuclear cytoplasmic aggregates classified as large. **C**, **D)** Motoneuronal cells containing both large perinuclear cytoplasmic aggregates and small neuropil aggregates: in **C**, soluble AR is also present in the cell nucleus; in **D**, the AR is excluded from the nucleus. Scale bar = 10 µm.

Fig. 5

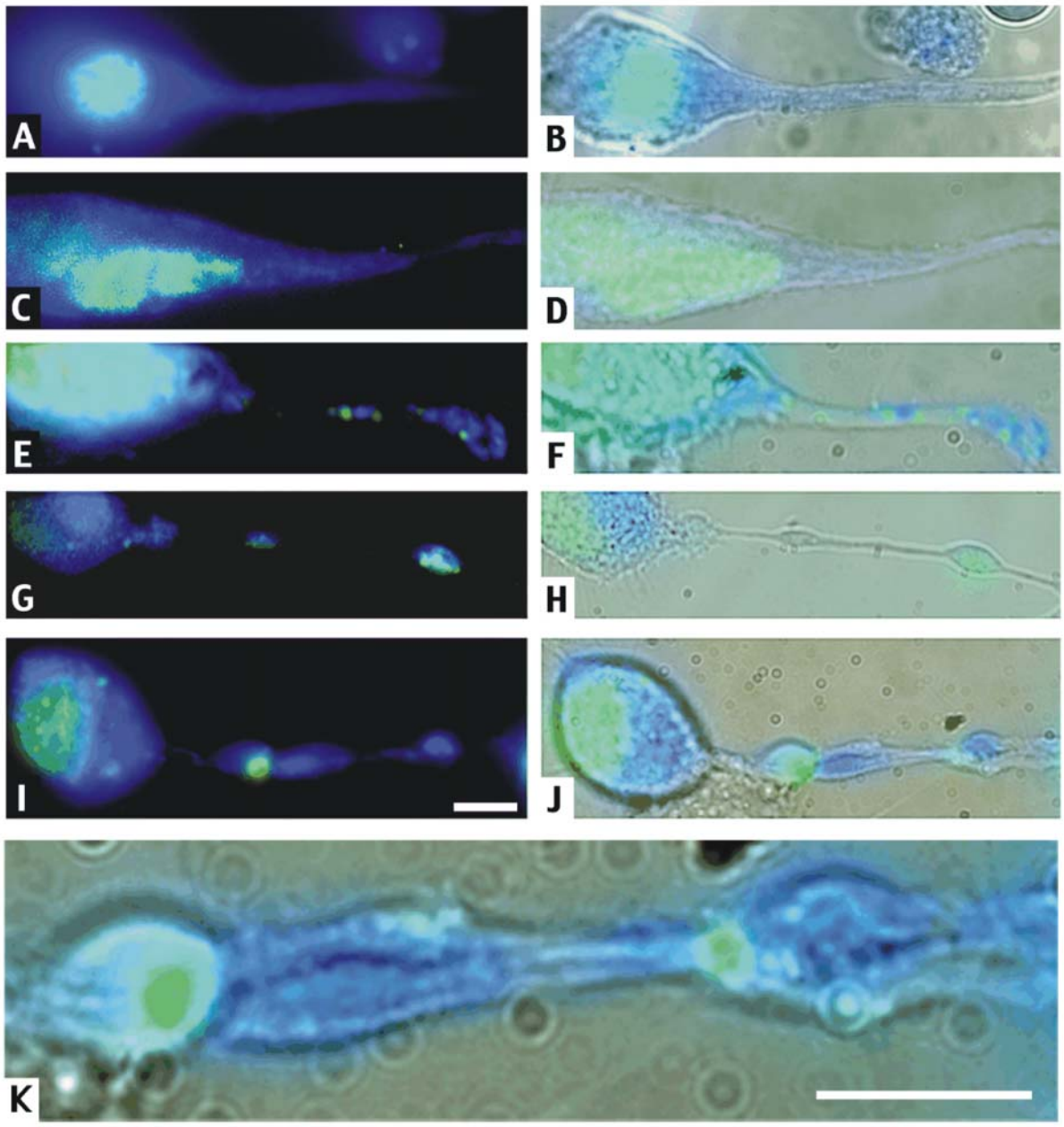

Figure 5. **Swelling of processes containing neuropil aggregates.** NSC34 cells were cotransfected with GFP-AR.Q(n)s proteins and mtBFP. Transfected cells were treated with testosterone. **A)** NSC34 cell expressing GFP-AR.Q0 (green) and mtBFP. **B)** Phase-contrast microscopy of the cell shown in *A*, used to visualize cell morphology and merged with the corresponding fluorescence analysis shown in *A*. **C)** NSC34 cell expressing GFP-AR.Q22 (green) and mtBFP. **D)** The results for **C** merged with the corresponding phase-contrast microscopic analysis to visualize cell morphology. **E**, **G**, **I)** NSC34 cells expressing GFP-AR.Q48 and bearing neuropil aggregates (green) and mtBFP (blue). *F*, *H*, *J*) The results for **E**, **G**, and **I** merged with phase-contrast microscopic analysis to visualize cell morphology. **E**, **F)** NSC34/GFP-AR.Q48/mtBFP cell bearing "jams" in the cell processes: mitochondria are entrapped by two small aggregates. The cell neurite appears unexpectedly large and constant in diameter, with a substantially normal phenotype. **G**, **H)** NSC34/GFP-AR.Q48/mtBFP cell: mitochondria and small AR aggregates: the accumulation of insoluble material results in abnormal and localized enlargements of the neurite accompained by an increased number of mitochondria in the swollen neurite. In *I* and *J*, an NSC34/GFP-AR.Q48/mtBFP cell shows a neurite swelling similar to that depicted in **G** and **H**, but this is apparently induced by the intersection of two processes arising from different cells. A higher magnification view of these two intersecting neurites appears in **K**. Scale bars = 10 µm.

Fig. 6

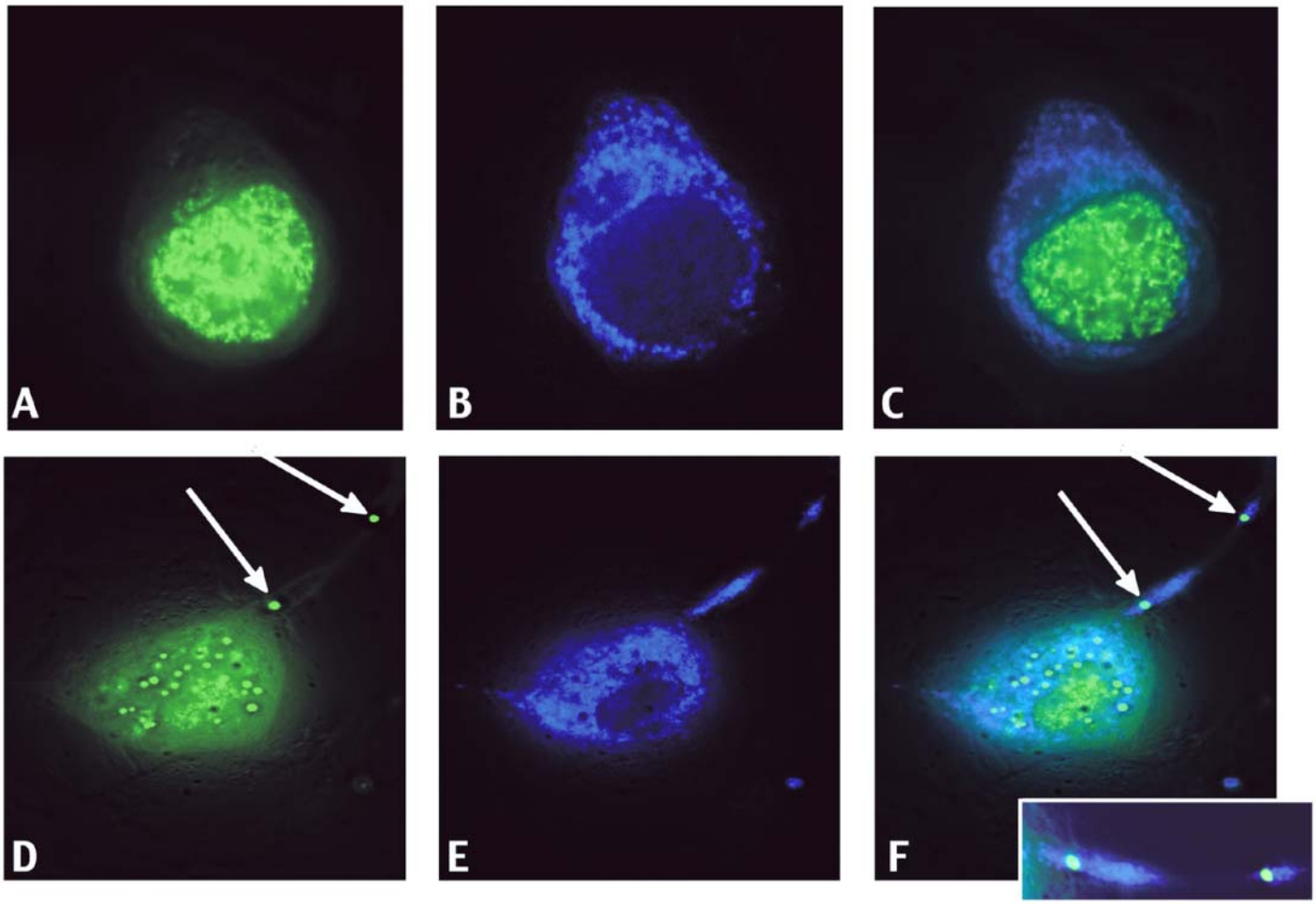

Figure 6. **Mitochondrial distribution in immortalized motoneuronal cells expressing ARs with elongated polyGlu tracts.** NSC34 cells were cotransfected with GFP-AR.Q(n)s proteins (Q0 or Q48) and mtBFP. **A**, **B**, **C)** NSC34 cells cotransfected with GFP-AR.Q0 and mtBFP after testosterone treatment: **A**, subcellular localization of GFP-AR.Q0; **B**, subcellular localization of mitochondria; **C**, merged analysis. **D**, **E**, **F)** NSC34 cells cotransfected with GFP-AR.Q48 and mtBFP after testosterone treatment: **D**, subcellular localization of GFP-AR.Q48 with aggregates in neurites (arrows); **E**, subcellular localization of mitochondria; **F**, merged analysis with aggregates in neurites and accumulation of mitochondria (arrows). The inset in **F** shows the neurite at higher magnification. Scale bar = 10 µm.

Fig. 7

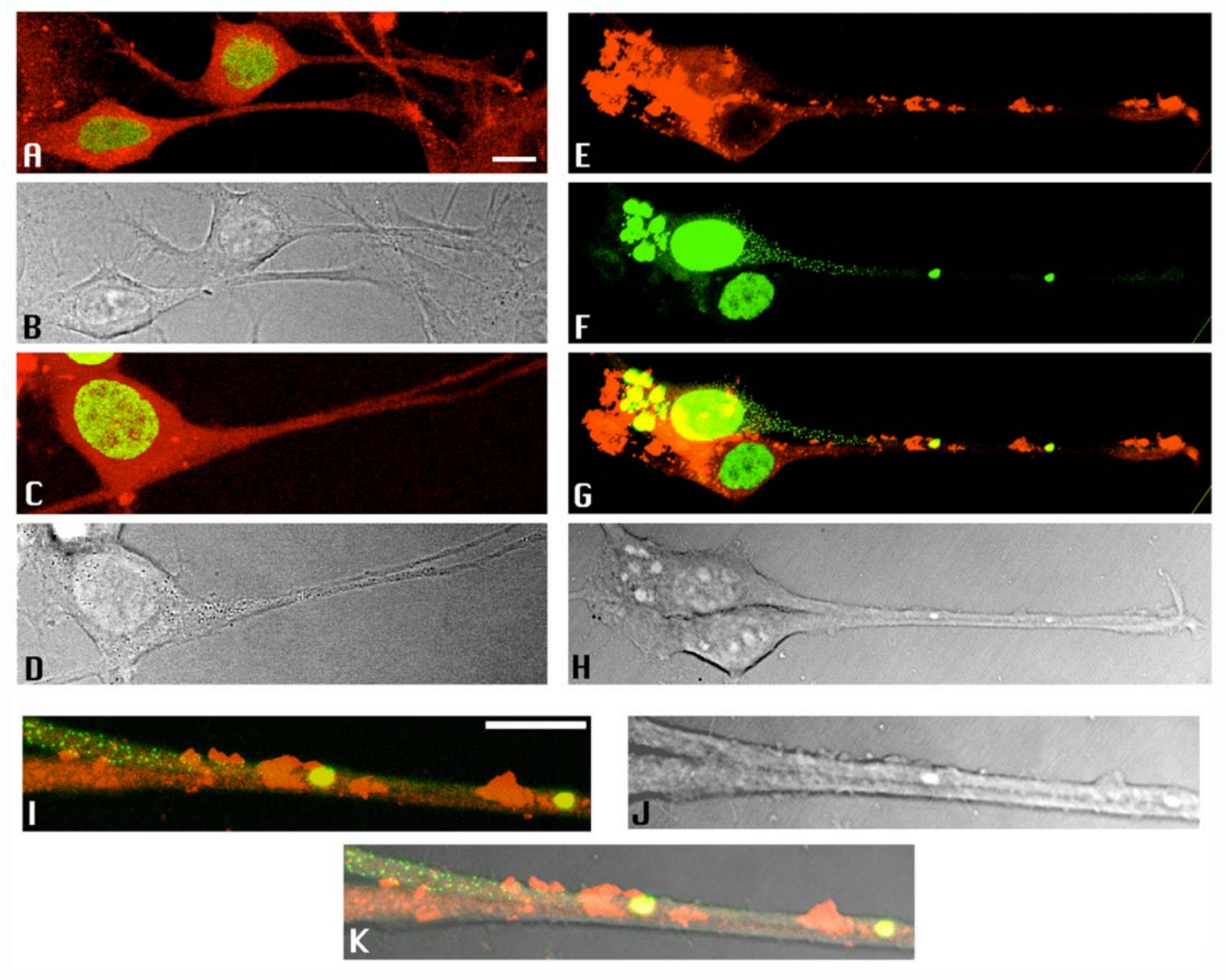

Figure 7. **Kinesin distribution in NSC34 cells containing neuropil aggregates.** NSC34 cells were transiently transfected with GFP-AR.Q(n)s and treated with testosterone. The cells were then processed by using an anti-kinesin monoclonal antibody (MAB1614, Chemicon) and visualized with a TRICT secondary antibody. **A)** Distribution of kinesin (red) in control GFP-AR.Q0 (green)-transfected NSC34 cells. **B)** Light-transmitted microscopy of cells in **A**. **C)** Distribution of kinesin (red) in control GFP-AR.Q22 (green)-transfected NSC34 cells. **D)** Light transmitted microscopy of cells in **C**. Images were obtained with a confocal fluorescence microscope. **E-H)** Analysis of GFP-AR.Q48-transfected cells. **E)** Kinesin immunoreactivity in two contiguous cells expressing GFP-AR.Q48. **F)** Fluorescence analysis to detect GFP-AR.Q48; both NSC34 cells were positive for AR, but only one contained neuropil aggregates. **G)** Merged analysis of **E** and **F**. **H)** Light transmission analysis of the same cells. **I**, **J)** Higher magnification of the neurites in **G** and **H** showing the region of the neurites containing the AR aggregates and kinesin accumulation. **K)** Merged analysis of **I** and **J**. Little distortion of the axonal caliber was observed in this case (**J**). Scale bar = 10 µm.